UNIVERSITY OF COPENHAGEN

Continuous measurements of nitrous oxide isotopomers during incubation experiments

Winther, Malte Nordmann; Balslev-Harder, David; Christensen, Søren; Priemé, Anders; Elberling, Bo; Crosson, Eric; Blunier, Thomas

Continuous measurements of nitrous oxide isotopomers during incubation experiments

Malte Winther[1], David Balslev-Harder[1,2], Søren Christensen[3], Anders Priemé[4,5], Bo Elberling[5], Eric Crosson[6], and Thomas Blunier[1]

[1]Centre for Ice and Climate, Niels Bohr Institute, University of Copenhagen, Denmark
[2]DFM - Danish National Metrology Institute, Kgs. Lyngby, Denmark
[3]Section for Terrestrial Ecology, Department of Biology, University of Copenhagen, Denmark
[4]Section for Microbiology, Department of Biology, University of Copenhagen, Denmark
[5]Center for Permafrost, Department of Geosciences and Natural Resource Management, University of Copenhagen, Denmark
[6]Picarro Inc, Santa Clara, CA 95054 USA

Correspondence to: Malte Winther (malte.winther@nbi.ku.dk)

Abstract. Nitrous oxide (N_2O) is an important and strong greenhouse gas in the atmosphere and part of a feed-back loop with climate. N_2O is produced by microbes during nitrification and denitrification in terrestrial and aquatic ecosystems. The main sinks for N_2O are turnover by denitrification and photolysis and photo-oxidation in the stratosphere. The position of the isotope ^{15}N in the linear N=N=O molecule can be distinguished between the central or terminal position (isotopomers of

5   N_2O). It has been demonstrated that nitrifying and denitrifying microbes have a different relative preference for the terminal and central position. Therefore, measurements of the site preference in N_2O can be used to determine the source of N_2O i.e. nitrification or denitrification. Recent instrument development allows for continuous (on the order of days) position dependent $\delta^{15}N$ measurements at N_2O concentrations relevant for studies of atmospheric chemistry. We present results from continuous incubation experiments with denitrifying bacteria, *Pseudomonas fluorescens* (producing and reducing N_2O) and *Pseudomonas*

10   *chlororaphis* (only producing N_2O). The continuous position dependent measurements reveal the transient pattern (KNO_3 to N_2O and N_2, respectively), which can be compared to previous reported site preference (SP) values. We find bulk isotope effects of -5.5 ‰ ± 0.9 for *P. chlororaphis*. For *P. fluorescens*, the bulk isotope effect during production of N_2O is -50.4 ‰ ± 9.3 and 8.5 ‰ ± 3.7 during N_2O reduction. The values for *P. fluorescens* are in line with earlier findings, whereas the values for *P. chlororaphis* are larger than previously published $\delta^{15}N^{bulk}$ measurements from production. The calculations of the SP

15   isotope effect from the measurements of *P. chlororaphis* result in values of -6.6 ‰ ± 1.8. For *P. fluorescens*, the calculations results in SP values of -5.7 ‰ ± 5.6 during production of N_2O and 2.3 ‰ ± 3.2 during reduction of N_2O. In summary, we implemented continuous measurements of N_2O isotopomers during incubation of denitrifying bacteria and believe that similar experiments will lead to a better understanding of denitrifying bacteria and N_2O turnover in soils and sediments and ultimately hands-on knowledge on the biotic mechanisms behind greenhouse gas exchange of the Globe.

20   **Keywords**

Nitrous oxide, isotopomers, site preference, greenhouse gas, denitrification, *Pseudomonas fluorescens*, *Pseudomonas chloro-raphis*, bacterial production, bacterial reduction

1 Introduction

The atmospheric concentration of nitrous oxide (N_2O) has increased from approximately 271 ppb before the industrialization to 324 ppb in 2011 [(Ciais et al., 2013)]. This increase has resulted in (1) an enhanced radiative forcing, e.g. N_2O has the third highest contribution to the radiative forcing of the naturally occurring greenhouse gasses [(Hartmann et al., 2013)], and (2) an increased production of nitrogen oxides (NOx) in the stratosphere and thereby an increased ozone-depletion. [(Forster et al., 2007); (Kim and Craig, 1993)]

Ice core records show that concentrations of N_2O correlates with northern hemispheric temperature variations, e.g. during the last glacial-interglacial termination as well as over the rapid climate variations occurring during the glacial period, known as Dansgaard-Oeschger events (D-O events). However, occasionally (e.g. D-O event 15 and 17) the N_2O concentration increases long before the onset of the dramatic temperature change Schilt et al. (2010), providing a potential early warning for rapid climate change. Isotopomers of N_2O provide information on the sources [(Clark, 1999)] and may improve our understanding on why N_2O is leading over some rapid climate change events. The stable isotopes of nitrogen are ^{14}N and ^{15}N with average isotopic abundances (mole-fraction) in the atmosphere of 0.99634 and 0.00366, respectively [(Junk and Svec, 1958)].

The N_2O molecule has an asymmetric linear structure (N=N=O) where the position of the ^{15}N can be discriminated. The isotopomers are named $^{15}N^{\alpha}$ and $^{15}N^{\beta}$ or short α and β for $^{14}N^{15}N^{16}O$ and $^{15}N^{14}N^{16}O$, respectively [(Yoshida and Toyoda, 2000)]. The two isotopomers cannot be distinguished directly by isotope ratio spectrometry, as they have the same mass. However, a distinction is possible using mid-infrared spectroscopy because the rotational and vibrational conditions are different for the two isotopomers providing regions where absorptions of the two isotopomers do not overlap. For isotopomer measurements at low N_2O concentration (low ppm range), a joint instrument development was executed, applying cavity ring down spectroscopy (CRDS) to enable continuous measurements (on the order of days) of the isotopomer abundances and yielding values for $^{15}N^{\alpha}$ and $^{15}N^{\beta}$.

For isotopomers, the isotopic composition is reported as delta values; the deviation of the elemental isotope ratio R from a standard (equation 1). The standard for nitrogen is today's atmospheric composition.

$$\delta^{15}N = \frac{R_{Sample}}{R_{Std}} - 1 \quad \text{where} \quad R = \frac{\left[^{15}N\right]}{\left[^{14}N\right]} \tag{1}$$

The N_2O bulk isotopic composition calculates as the average of $\delta^{15}N^{\alpha}$ and $\delta^{15}N^{\beta}$ while the site preference (SP) is defined as their difference ($\delta^{15}N^{SP} = \delta^{15}N^{\alpha} - \delta^{15}N^{\beta}$). [(Brenninkmeijer and Röckmann, 1999); (Park et al., 2011); (Toyoda et al., 2002)].

$$\delta^{15}N^{bulk} = \frac{\delta^{15}N^{\alpha} + \delta^{15}N^{\beta}}{2} \tag{2}$$

There are multiple natural and anthropogenic sources of N_2O. The primary anthropogenic sources of N_2O are fertilizers including nitrogen minerals used for agriculture. The natural sources are primarily nitrification and denitrification in terrestrial

and aquatic ecosystems. [(Mosier et al., 1998); (Olivier et al., 1998)].

Denitrification is a stepwise biological reduction process in which denitrifying bacteria produce nitrogen (N_2). Under anaerobic conditions the denitrifying bacteria use nitrate (NO_3^-) instead of oxygen as an electron acceptor in the respiration of organic matter. Through multiple anaerobic reactions N_2 is produced as the end product of the complete denitrifying process (reaction

5   R1) [(Firestone and Davidson, 1989)].

$$NO_3^- \rightarrow NO_2^- \rightarrow NO \rightarrow N_2O \rightarrow N_2 \tag{R1}$$

Each of these anaerobic reactions is carried out by a genuine enzyme, i.e., the production of N_2O is caused by the reaction between nitric oxide (NO) and the enzyme nitric oxide reductase (NOR). The NOR enzyme works as a catalyst in the reduction of NO as shown in equation R2. [(Wrage et al., 2001); (Tosha and Shiro, 2013)]

10   $$2NO + 2e^- + 2H^+ \rightarrow N_2O + H_2O \tag{R2}$$

Reactions with different enzymes typically result in specific isotopic fractionation. The isotope fractionation of the intermediately produced N_2O during denitrification is a consequence of multiple reaction steps i.e., the isotope fractionation is determined as product-to-substrate fractionation. Two species of denitrifying bacteria with slightly different enzymes potentially leads to different fractionation. In this study, we compared the fractionation of N_2O by two contrasting denitrifying

15   bacteria; *Pseudomonas fluorescens* producing and reducing N_2O, and *Pseudomonas chlororaphis* producing but not reducing N_2O. We hypothesized that these contrasting denitrifying bacteria show differences in isotope enrichment and SP during N_2O production and reduction.

2   Method

Our objective was to perform continuous position dependent $\delta^{15}N$ measurements of two different bacterial cultures during in-

20   cubation experiments. Using two denitrifying bacterial cultures we determine the isotope enrichment and SP during production and reduction of N_2O, respectively.

2.1   Instrumentation

Bacterial production of N_2O was continuously measured by mid-infrared cavity ringdown spectrometry using a prototype of the Picarro G5101-i analyzer (in the following named G5101i-CIC) (Picarro, Santa Clara, California, USA). The measurements

25   are non-destructive and are therefore suitable for incubation experiments. The CRDS instrument measures the ^{14}N, $^{15}N^\alpha$ and $^{15}N^\beta$ absorption features of N_2O in the wavelength region between 2187.4 cm^{-1} and 2188 cm^{-1}. The typical precision of the instrument is 1 ppb for the N_2O mixing ratio and 5.2 ‰ for each of the delta values of the two isotopomers [(Balslev-Clausen, 2011)].

Measurements are made by placing the sample delivery system of the G5101i-CIC in a closed loop with a microbial incubation

30   glass chamber (Fig. 1). Circulation is provided by a "leak-reduced" diaphragm pump installed downstream from the analyzer.

The pump (KNF N84.4 ANE) has been sealed using vacuum sealant (Celvaseal high vacuum leak sealant, Myers vacuum repair service, Inc., Kittanning, PA 16201, USA). A low leak rate is prerequisite for accurate measurements in a closed loop experiment. Before the analyzer, a Nafion unit and an "Ascarite" trap is installed. The Nafion unit removes H_2O vapor whereas the Ascarite trap chemically removes CO_2. Both gasses are removed to exclude potential spectral interference with N_2O in the

5 cavity of the analyzer. Underneath the glass chamber a magnetic stirrer is installed. The stirrer serves two purposes 1) ensure a complete mixing of the bacterial solution and the added nutrient, i.e. potassium nitrate (KNO_3^-), and 2) facilitate gas exchange.

In addition to the measuring mode, the system can be flushed with N_2 (not shown in Fig. 1). The flushing mode is used to obtain an anaerobic starting point of the incubation experiment free of N_2O. The flushing procedure is fully automated

10 to ensure reproducibility. The entire incubation setup is flushed with N_2 for 310 seconds at a high flow rate. The resulting overpressure in the incubator is released prior to switching back to the closed loop position.

2.2 Correction of CRDS concentration dependence

Isotope measurements made with the G5101i-CIC have a N_2O concentration dependence and need to be corrected. A concentration dependent correction is required because there is a 1/concentration dependence, caused by small offsets in the

15 measurement of the ^{14}N - ^{15}N - ^{16}O and ^{15}N - ^{14}N - ^{16}O peaks. These offsets are caused by baseline ripple created by optical cavity etalons. An etalon is an optical effect in which a beam of light undergoes multiple reflections between two reflecting surfaces, and whose resulting optical transmission or reflection is periodic in wavelength. The ripples are not always constant in phase, which means that the ripples can shift spectrally, which can cause the offset to drift over time. The result is a concentration dependent error to δ of the form $\pm$ 1/concentration. Because baseline ripple effects become more dominant as N_2O

20 concentration decreases, the "relative" error is largest at low concentrations.
Figure 2 shows results from a dilution experiment where we gradually mixed a pure N_2O gas with a N_2/O_2 mixture (20.1 % O_2 and 79.9 % N_2, purity 99.999 %). Measurements were performed in a 60 minutes stepwise sequence of both increasing and decreasing concentrations.

25 We chose to fit the raw data with a cubic spline smoothing function (CSS-function) [(Brumback and Rice, 1998)]. The best fit of these CSS-functions are found using a smoothing parameter of p = 0.999 in a regression analysis. Four outliers were identified to be outside the 2σ boundary and removed from the data set (the red circles in Fig. 2). After these outliers were removed the best fit was found again and the concentration dependent correction was applied as shown with the green profiles in Fig. 2. Over the course of the experiments, no further instrumental drift was observed.

30 ### 2.3 Calibration gases

Working standards for N_2O bacterial incubations are CIC-MPI-1 and CIC-MPI-2. The two standard gasses were prepared based on two standard gasses provided by J. Kaiser at University of East Anglia (UEA), Norwich, United Kingdom. These standard gasses, MPI-1 and MPI-2, are pure N_2O gasses with different isotopic composition [(Kaiser, 2002)]. In our laboratory,

each of the standard gasses was diluted with a N_2/O_2 mixture (20.1 % O_2 and 79.9 % N_2, purity 99.999 %) resulting in the two new standard gasses, CIC-MPI-1 and CIC-MPI-2. Both CIC-standard gasses were measured at four different laboratories to ensure consistent isotopic values according to an international standard reference. The gasses were measured at Tokyo Institute of Technology in Japan, at Institute for Marine and Atmospheric research Utrecht in The Netherlands (IMAU), at the Centre for Ice and Climate in Copenhagen, Denmark (CIC), and originally at University of East Anglia in Norwich, United Kingdom (UEA). At Tokyo-Tech, three GC/IRMS measurements of each CIC-MPI gas resulted in an average $\delta^{15}N^{\alpha}$ = 1.44 ‰ ± 0.09 and an average $\delta^{15}N^{\beta}$ = 1.24 ‰ ± 0.35 for CIC-MPI-1, and for CIC-MPI-2 the measurements resulted in average $\delta^{15}N^{\alpha}$ = 12.79 ‰ ± 0.22 and $\delta^{15}N^{\beta}$ = -15.41 ‰ ± 0.24. At IMAU 22 GC/IRMS measurements of each CIC-MPI gas resulted for CIC-MPI-1 in $\delta^{15}N^{\alpha}$ = 2.30 ‰ ± 0.25 and $\delta^{15}N^{\beta}$ = -0.16 ‰ ± 0.33, and for CIC-MPI-2 in $\delta^{15}N^{\alpha}$ = 11.79 ‰ ± 0.37 and $\delta^{15}N^{\beta}$ = -15.16 ‰ ± 0.46. At CIC each CIC-MPI gas was continuously measured over two hours. The average results for CIC-MPI-1 was $\delta^{15}N^{\alpha}$ = 0.53 ‰ ± 2.61 and $\delta^{15}N^{\beta}$ = 4.95 ‰ ± 3.57, and for CIC-MPI-2 in $\delta^{15}N^{\alpha}$ = 12.58 ‰ ± 2.75 and $\delta^{15}N^{\beta}$ = -12.89 ‰ ± 3.21. All measurements were performed relative to atmospheric air and our position dependent $\delta^{15}N$ measurements are therefore well referenced to atmospheric air. An average of the concentrations and the isotopic compositions of the two new standard gasses are specified (Table 1).

2.4 Pure bacterial cultures

The two bacterial cultures used in this study are both gram-negative bacteria with the capability to denitrify, i.e. reduce nitrate to gaseous nitrogen. Isolates were obtained from an agricultural soil of sandy loam type (Roskilde Experimental Station) on 11 April 1983. One culture is a *Pseudomonas fluorescens*, bio-type D that reduces NO_3^- all the way to N_2. The second culture, *Pseudomonas chlororaphis*, is only capable of reducing NO_3^- to N_2O [(Christensen and Bonde, 1985)], which means that the nitrous oxide reductase is absent or at least not active in this organism. The latter bacterium is contained in the American Type Culture Collection with accession number ATCC 43928 [(Christensen and Tiedje, 1988)]. The cultures were grown anoxic in 50 ml serum bottles with 1/10 tryptic soy broth (Difco) added 0.1 g $KNO_3 \cdot L^{-1}$. After six days of growth at room temperature (24 °C), *P. chlororaphis* had reduced all N in NO_3^- into N_2O. The bacterial culture of *P. Fluorescens* was cultivated for six days at a slightly lower temperature (15 °C) to assure that the cultures were in a comparable phase of potential activity when assayed for gas production/reduction activity. The six days old cultures were used in the incubation experiment in which it is conditional for the denitrifying process that organic carbon is available, that the concentration of oxygen is low and that the concentration of NO_3^- is high [(Wrage et al., 2001); (Stuart Chapin III et al., 2002)].

2.4.1 Bacterial incubation experiments

50 mL bacterial solution of *P. chlororaphis* or *P. fluorescens* was placed in a petri-dish in the 1000 mL incubation chamber. Hereafter, the setup was flushed with pure N_2 (purity 99.9999 %) to ensure anaerobic conditions. To ensure no N_2O gas exchange prior to the experiment, the bacterial solution was left for 90 minutes under constant magnetic stirring. Then the incubation chamber was opened and the bacterial solution was fed with 2.5 mL and 15 mL 0.45 mM KNO_3 for *P. chlororaphis* and *P. fluorescens*, respectively. The incubation experiment started by again flushing the setup with pure N_2 immediately after

the addition of KNO_3.

A total of seven replicate incubations of the full denitrifying bacteria (*P. fluorescens*) and five replicate incubations of the denitrifying bacteria with no active nitrous oxide reductase (*P. chlororaphis*) were assessed. All of the cultures were continuously measured from the moment KNO_3 was added to the bacterial incubations. The experiment with *P. fluorescens* was terminated

5 when the N_2O concentration was below 0.2 ppm. For *P. chlororaphis*, we defined the end of the experiment when the N_2O concentration had reached a constant level for 200 minutes.

The CIC-MPI gasses are based on a N_2/O_2 mixture where the incubation measurements are based on N_2. This difference does not affect the results since no O_2 spectral lines exist in the wavelength region set in the G5101i-CIC.

2.5 Analysis of isotope enrichment

10 The observed isotope changes in N_2O during our incubation experiment can be analyzed in terms of Rayleigh fractionation. Rayleigh fractionation describes the changing isotopic composition in reactant and product of a unidirectional reaction. Equation 3 gives the isotope ratio of the reactant as:

$$\frac{R_s}{R_{s,0}} = f^{\left(\alpha_{p/s}-1\right)}$$
(3)

where $R_{s,0}$ is the initial isotope ratio of the reactant, R_s is the isotope ratio of the product at time t, $\alpha_{p/r}$ is the fractionation factor

15 of the product versus the substrate, and f is the unreacted fraction of substrate at time t. The isotope enrichment calculates as ϵ = $\alpha - 1$ from the fractionation factors in equation 3. We do not measure the isotopic composition of KNO_3 in our experiments. However, by definition the end values of N_2O for *P. chlororaphis* when all KNO_3 has reacted has to be identical to the initial value of KNO_3.

The Rayleigh type distillation is valid for the bulk isotope ratios of N_2O. The corresponding equation for the accumulated

20 product is:

$$R_{p,acc}^{bulk} = R_0 \cdot \left(\frac{1 - f^{\alpha_{bulk}}}{1 - f}\right)$$
(4)

The isotope enrichment for the bulk can be described using the isotope enrichment of the product ([(Menyailo and Hungate, 2006); (Ostrom et al., 2007); (Mariotti et al., 1981); (Lewicka-Szczebak et al., 2014)]).

$$\epsilon_{p,acc}^{bulk} = (\alpha_{bulk} - 1)$$
(5)

25 The described Rayleigh equation is not directly applicable to the isotopomers, as these are both direct products of the same denitrification process from the same batch of denitrifying bacteria and nitrate. An isotopomer correction factor derives to φ_α and φ_β for the two isotopomers respectively.

$$\varphi_\alpha = 1 + \left(\frac{\alpha_\beta - \alpha_\alpha}{2}\right)$$
(6)

30 $$\varphi_\beta = 1 - \left(\frac{\alpha_\beta - \alpha_\alpha}{2}\right)$$
(7)

The Rayleigh equation for the accumulated product of an isotopomer is therefore:

$$R_{p,acc}^{isotopomer} = R_{p,acc}^{bulk} \cdot \varphi \tag{8}$$

Equation 8 is valid for *P. chlororaphis*. For *P. fluorescens*, both an immediate reduction and an uptake reduction take place simultaneously with N_2O production due to the pre-experimental cultivation leading to activation of all enzymes in the bacterial solution. Part of the freshly produced N_2O is therefore immediately reduced to N_2. This reduction is fractionating with fractionation factor α_R. The isotope imprint of the reduction on the remaining N_2O depends on the ratio between reduction and production rate (γ). Assuming γ is constant results in the following first order approximation.

$$R_{p,r} = \frac{R_{p,acc} \cdot (1 - \alpha_R \cdot \gamma)}{1 - \gamma} \tag{9}$$

$$R_{p,r,acc} = \frac{R_{p,r} \cdot f \cdot (1 - \gamma)}{f \cdot (1 - \gamma)} \tag{10}$$

For any calculated ratio the values are given in ‰ using the delta-notation (equation 1).

The SP of N_2O, being the difference between the $\delta^{15}N^\alpha$ and $\delta^{15}N^\beta$, is not compatible to the Rayleigh equations. Applying the assumption that $\delta_{s,0} << 1000\,‰$, the isotope enrichment simplifies to $\epsilon_{p/s} \approx \delta_p - \delta_s$, such that e.g., $\epsilon_\alpha = (\delta^{15}N^\alpha - \delta^{15}N^{NO_3})$. For SP, the isotope enrichment is therefore given as $\epsilon_{sp} = \epsilon_\alpha - \epsilon_\beta$, which derives to ([[Menyailo and Hungate, 2006); (Ostrom et al., 2007); (Mariotti et al., 1981); (Lewicka-Szczebak et al., 2014)]):

$$\epsilon_{SP} = \delta^{15}N^\alpha - \delta^{15}N^\beta \tag{11}$$

2.5.1 Application of Rayleigh model

We determine the respective isotope enrichment during production and reduction of N_2O for each of the bacterial strains assuming a Rayleigh type process. The Rayleigh distillation model is fitted to the δ-value and the N_2O concentration data. As *P. chlororaphis* is a pure producer of N_2O this is straight forward. For *P. fluorescens* the section of production is defined as being from the start of the measurements until the end of net production. From the calculations of the production rates (see Fig. 3) we believe that N_2O production continues after the point of maximum concentration. Therefore the unreacted fraction at the end of net production is iteratively found and is > 0. Other parameters that are iteratively found are the fractionation factor between $\alpha = 0$ and $\alpha = 1$ and the reduction to production rate γ (between 0 and 1). The fractionation factors resulting in the highest R^2 values was picked as the correct fractionation factor for each specific evolution. Production of N_2O by *P. fluorescens* continues past the point of net production. However, at one point NO_3^-, NO_2^- and NO are fully consumed and *P. fluorescens* is forced to exclusively reduce N_2O. We defined the start of the section where *P. fluorescens* is only reducing N_2O to the point where both $\delta^{15}N^\alpha$ and $\delta^{15}N^\beta$ start decreasing. Between the end of the net production and the start of the exclusive reduction, no Rayleigh model can be fitted.

The models are fitted using both the CDC data and the 5 minutes running mean of the CDC data. The best fit is found using

an iterative approach of the R^2 value between the measured data and the Rayleigh distillation equation for the accumulated product (equation 8 and equation 10 for *P. chlororaphis* and *P. fluorescens*, respectively). Iterative calculations are performed for fractionation factor between $\alpha = 0$ and $\alpha = 1$ during production of N_2O, and between $\alpha = 1$ and $\alpha = 2$ during reduction of N_2O. The reduction correction parameter (γ) is iteratively determined to be between $\gamma = 0$ and $\gamma = 1$. The fractionation factors resulting in the highest R^2 values are picked as the correct fractionation factor for each specific evolution.

3 Results

The evolution of N_2O over time from the two bacterial strains shows two very distinctive patterns with both an increasing and decreasing N_2O concentration characteristic for *P. fluorescens* and an increasing N_2O concentration followed by a stabilization characteristic for *P. chlororaphis* (Fig. 3A) as has previously been described by Christensen and Tiedje (1988). These distinctive characteristics are only vaguely seen in the respective dynamics of the SP for the two bacterial strains (Fig. 4A, 4B, 5A and 5B).

3.1 Pseudomonas chlororaphis

Paralleling the increase in N_2O concentration (Fig. 3A), we also find an increase in $\delta^{15}N^\alpha$, $\delta^{15}N^\beta$ and $\delta^{15}N^{bulk}$ over time (Fig. 4A and 4B). The final product of *P. chlororaphis* is N_2O; this is a unidirectional transfer of nitrogen from KNO_3 to N_2O and thereby a Rayleigh process although multiple fractionations are involved. In Fig. 4A and 4B, we plot the best fit Rayleigh profile for $\delta^{15}N^\alpha$ and $\delta^{15}N^\beta$ respectively.

The modeled Rayleigh distillation profiles were found to match the production of N_2O from *P. chlororaphis* to a relatively high degree. The average correlation coefficients (R^2) between data and fitted Rayleigh curves are 0.709, 0.654, and 0.767 for $\delta^{15}N^\alpha$, $\delta^{15}N^\beta$ and $\delta^{15}N^{bulk}$ respectively. The calculations of the isotope enrichment for the fractionation of $\delta^{15}N^\alpha$ give a mean value of -8.8 ‰ ± 1.4. For $\delta^{15}N^\beta$ the mean enrichment factor was found to be -2.2 ‰ ± 1.1 (Table 4). These values leads to a mean SP value of -6.6 ‰ ± 1.8 and a $\delta^{15}N^{bulk}$ enrichment factor of -5.5 ‰ ± 0.9.

3.2 Pseudomonas fluorescens

Continuous measurements of the evolution of N_2O produced and consumed by the denitrifying bacteria *P. fluorescens* are presented in Fig. 5A and 5B for the $\delta^{15}N^\alpha$ and $\delta^{15}N^\beta$, respectively. The correlation coefficient of the fitted apparent Rayleigh model for the production matches the continuously measured $\delta^{15}N^\alpha$ data by 94.1 % on average using the R^2 method for the seven replicates of *P. fluorescens* incubations. Equivalent R^2 average for $\delta^{15}N^\beta$ are 88.7 %, whereas the average for $\delta^{15}N^{bulk}$ are found to be 94.8 %. The R^2 found for the reduction part for the two isotopomers and the bulk is 91.3 % for $\delta^{15}N^\alpha$, 76.3 % for $\delta^{15}N^\beta$, and 91.7 % for $\delta^{15}N^{bulk}$ on average for the seven replicates. The fractionation during both the production and the reduction are therefore following the apparent Rayleigh type distillation to a large degree. The isotope enrichment calculated using these models are therefore a good representation for the fractionation caused by the *P. fluorescens* bacteria on the N_2O. The resulting isotope enrichment is presented in Table 2 for the production part and in Table 3 for the reduction part together

with the calculated isotope enrichment for the SP. During production of N_2O, the mean enrichment for SP was found to be ϵ_{SP} = -5.7 ‰ $\pm$ 5.6 while the ϵ_{bulk} = -50.4 ‰ $\pm$ 9.3 for the bulk, hence there is a difference of 44.9 ‰ and 0.8 ‰ for ϵ_{SP} and ϵ_{bulk}, respectively, to *P. chlororaphis*. During reduction of N_2O the mean enrichment for SP was found to be ϵ_{SP} = -2.3 ‰ $\pm$ 3.2 and ϵ_{bulk} = 8.5 ‰ $\pm$ 3.7 for the bulk.

5 4 Discussion

The two bacteria investigated are denitrifiers, i.e. functionally similar but with *P. chlororaphis* lacking the ability to reduce N_2O to N_2. Both denitrifiers were cultivated under anaerobic conditions leading to active nitric oxide reductase (both cultures) and nitrous oxide reductase (*P. chlororaphis*). This leads to a pre-experimental expectation that when fed the same amount of nitrate the maximum N_2O concentration and the N_2O production rate should be lower for *P. fluorescens* than for *P. chlororaphis*.

10 In Fig. 3, an example of the N_2O evolution by the two bacterial strains is plotted as the concentration of N_2O and the production rate versus time. Starting at time zero and moving with the profiles forward in time, the concentration of N_2O produced by *P. chlororaphis* has a higher production rate and reaches a higher level in concentration than that produced by *P. fluorescens* even though *P. fluorescens* received six times more nutrients than *P. chlororaphis*. These observations indicate that the nitrous oxide reductase consumes N_2O from a very early stage of the N_2O turnover, likely because the cultures were grown under

15 anaerobic conditions leaving both N_2O-producing and -consuming enzymes active from the beginning of the experiment.
N_2O produced by the two denitrifying bacteria differs in the bulk isotope enrichment whereas the SP enrichments are averaging to similar values. From the presented experiments we have found that the difference in enrichment between *P. chlororaphis* and *P. fluorescens* on average is 44.9 ‰ and 0.8 ‰ for ϵ_{bulk} and ϵ_{SP} respectively (Fig. 6). We therefore find that the isotopomers produced by *P. fluorescens* are more depleted than those produced from *P. chlororaphis*, since the Rayleigh is calculated as

20 product-to-substrate fractionation. Sutka and Ostrom (2006) conclude that a difference in the nitrite reductase does not have an effect on the SP during denitrification. This conclusion is based on measurements of *P. chlororaphis* (ATCC 43928) and *P. aureofaciens* (ATCC 13985) possessing cd1-type nitrite reductase and Cu-containing nitrite reductase, respectively. We conclude the same for *P. fluorescens* and *P. chlororaphis* and therefore propose that the conclusion applies to all denitrifying bacteria.
The observed difference in the isotope enrichment during production of N_2O could originate from a difference in the nitric

25 oxide reductase enzymes. Nitric oxide reductase is the primary enzyme in a chain of catalytic reactions leading to the production of N_2O [(Hino et al., 2010);(Hendriks et al., 2000)]. The catalytic cycle involving production of N_2O from NO has yet to be completely understood with respect to the formation of the N-N double bond, the complexity of the structural information of nitric oxide reductase, the proton transfer pathway into nitric oxide reductase [(Tosha and Shiro, 2013)], and the very short lifetime of the intermediate states of the molecules [(Collman et al., 2008)]. We hypothesized that the difference in the bulk ob-

30 served during incubation of our two bacterial species was due to different nitric oxide reductases produced by the two species. To test this hypothesis, we compared the DNA sequences of the norB and norC genes coding for the large and small subunit, respectively, of nitric oxide reductase from three different strains of *P. fluorescens* (strains NCIMB 11764 [Genbank accession number CP010945], PA3G8 [742825335], and F113 [CP003150]) and *P. chlororaphis* (strains O6 [389686655], PA23

[749309655], and UFB2 [836582503]) as well as two closely related denitrifying species, *P. aeruginosa* and *P. stutzeri*. Our analysis revealed 1) a very high similarity of the two genes in *P. fluorescens* and *P. chlororaphis* and 2) that the intra-species variability of the two genes was similar to the inter-species variation. This led us to reject our hypothesis and conclude that differences in nitric oxide enzymes produced by the two species were not responsible for the observed differences in the bulk.

5 We hypothesized that the difference in the bulk isotope enrichment between the two bacteria originates from mass-dependent fractionation associated with the nitrous oxide reductase in *P. fluorescens*. After production of N_2O molecules, the light molecules degas quickly out of the liquid phase and away from the nitrous oxide reductase. The heavy N_2O molecules are slower and react with the nitrous oxide reductase leading to a depletion of the heavy N_2O isotopes. As this is a diffusion driven process it is mass-dependent with no detectable effect on SP.

10 ## 4.1 Comparison to previous studies

Numerous publications have presented experiments with both in situ measurements of denitrifying bacterial production and reduction of N_2O during incubation of bacterial cultures and soil samples. In Fig. 6, we present a comparison between the results from this study and the results from a selection of the previously published results. The general understanding is that denitrification results in SP $\leq$ 10 ‰. Applying different incubation techniques on soils with different properties showed SP

15 during production of N_2O between -3 ‰ and 9 ‰ and between -2 ‰ and -8 ‰ during reduction [(Lewicka-Szczebak et al., 2014);(Well and Flessa, 2009a, b)]. During production of N_2O in bacterial culture experiments involving *P. chlororaphis* (ATCC 43928) and *P. aureofaciens* (ATCC 13985), Sutka and Ostrom (2006) found SP values of -2.5 ‰ and 1.3 ‰ and $\delta^{15}N^{bulk}$ values of between -7 ‰ and -10 ‰. Ostrom et al. (2007) investigated bacterial reduction of N_2O using *P. stutzeri* (provided by J. M. Tiedje) and *P. denitrificans* (ATCC 13867), and the SP resulting from this bacterial reduction of N_2O was

20 between -6.8 ‰ and -5 ‰.

Our results for N_2O SP and bulk enrichment from *P. chlororaphis* are in the same range as what has been reported previously. Measurements of *P. fluorescens* on the other hand show more depleted bulk enrichment values while the SP enrichment is in line with previous results. For the reduction of N_2O both measurements of the bulk isotope enrichment and SP are in line with

25 earlier results.

5 Conclusions

We have presented successful continuous measurements of the denitrifying bacterial process using two different strains of bacteria: *P. fluorescens* which is a full denitrifier, and *P. chlororaphis* which is a denitrifier without nitrous oxide reductase activity. Assuming a Rayleigh type fractionation, modified for isotopomers and simultaneous reduction, we have calculated the

30 isotope enrichment during production and reduction of N_2O. The enrichment for *P. chlororaphis* is in line with previous results for both SP and bulk. For *P. fluorescens*, we find similar SP enrichment values during N_2O production and reduction. The bulk

isotope enrichment calculated for N_2O reduction is in line with previously presented results though for production we find an isotope depletion. We believe that, in our experiment, the bulk isotope depletion is due to mass-dependent fractionation.

References

Balslev-Clausen, D. M.: Application of cavity ring down spectroscopy to isotopic bio- geo- & climate-sciences & the development of a mid-infrared CRDS analyzer for continuous measurements of N2O isotopomers, Ph.D. thesis, University of Copenhagen, 2011.

Brenninkmeijer, C. A. M. and Röckmann, T.: Mass spectrometry of the intramolecular nitrogen isotope distribution of environmental nitrous oxide using fragment-ion analysis, Rapid communications in mass spectrometry : RCM, 13, 2028–33, doi:10.1002/(SICI)1097-0231(19991030)13:20<2028::AID-RCM751>3.0.CO;2-J, 1999.

Brumback, B. a. and Rice, J. a.: Smoothing spline models for the analysis of nested and crossed sampes of curves, Journal of the American Statistical Association, 93, 961–994, 1998.

Christensen, S. and Bonde, G. J.: Seasonal variation in numbers and activity of denitrifier bacteria in soil. Taxonomy and physiological groups among isolates, Danish Journal of Plant and Soil Science, 89, 367–372, 1985.

Christensen, S. and Tiedje, J. M.: Sub-parts-per-billion nitrate method: Use of an N2O-producing denitrifier to convert NO3- or 15NO3- to N2O, Applied and environmental microbiology, 54, 1409–1413, 1988.

Ciais, P., Sabine, C., Bala, B., Bopp, L., Brovkin, V., Canadell, J., Chhabra, A., DeFries, R., Galloway, J., Heimann, M., Jones, C., Le Quéré, C., Myneni, R., Piao, S., and Thornton, P.: 6: Carbon and Other Biogeochemical Cycles, in: Carbon and Other Biogeochemical Cycles. In: Climate Change 2013: The Physical Science Basis. Contribution of Working Group I to the Fifth Assessment Report of the Intergovernmental Panel on Climate Change [Stocker, T.F., Qin, D., Plattner, G.-K., Tignor,, pp. 465–570, Cambridge University Press, Cambridge, United Kingdom and New York, NY, USA, doi:10.1017/CBO9781107415324.015, 2013.

Clark, P. U.: Northern Hemisphere Ice-Sheet Influences on Global Climate Change, Science, 286, 1104–1111, doi:10.1126/science.286.5442.1104, 1999.

Collman, J. P., Yang, Y., Dey, A., Decréau, R. A., Ghosh, S., Ohta, T., and Solomon, E. I.: A functional nitric oxide reductase model., Proceedings of the National Academy of Sciences of the United States of America, 105, 15 660–5, doi:10.1073/pnas.0808606105, 2008.

Firestone, M. K. and Davidson, E. A.: Microbiological basis of NO and N2O production and consumption in soil., Exchange of Trace Gases between Terrestrial Ecosystems and the Atmosphere, pp. 7–21, 1989.

Forster, P., Ramaswamy, V., Artaxo, P., Berntsen, T., Betts, R., Fahey, D., Lean, J. H. J., Lowe, D., Myhre, G., Prinn, J. N. R., Raga, G., Schulz, M., and Dorland, R. V.: Climate Change 2007: The Physical Science Basis. Contribution of Working Group I to the Fourth Assessment Report of the Intergovernmental Panel on Climate Change, chapter Changes in Atmospheric Constituents and in Radiative Forcing, Cambridge University Press, Cambridge, United Kingdom and New York, NY, USA., pp. 130–217, 2007.

Hartmann, D., Klein Tank, A., Rusticucci, M., Alexander, L., Brönnimann, S., Charabi, Y., Dentener, F., Dlugokencky, E., Easterling, D., Kaplan, A., Soden, B., Thorne, P., Wild, M., and Zhai, P.: 2: Observations: Atmosphere and Surface, in: 2013: Observations: Atmosphere and Surface. In: Climate Change 2013: The Physical Science Basis. Contribution of Working Group I to the Fifth Assessment Report of the Intergovernmental Panel on Climate Change, edited by Stocker, T., Qin, D., Platter, G.-K., Tignor, M., Allen, S., Boschung, J., Nauels, A., Xia, Y., Bex, V., and Midgley (eds.), P., Cambridge University Press, Cambridge, United Kingdom and New York, NY, USA, 2013.

Hendriks, J., Oubrie, A., Castresana, J., Urbani, A., Gemeinhardt, S., and Saraste, M.: Nitric oxide reductases in bacteria., Biochimica et biophysica acta, 1459, 266–273, doi:10.1016/S0005-2728(00)00161-4, 2000.

Hino, T., Matsumoto, Y., Nagano, S., Sugimoto, H., Fukumori, Y., Murata, T., Iwata, S., and Shiro, Y.: Structural Basis of Biological N2O Generation by Bacterial Nitric Oxide Reductase, Science, 330, 1666–1670, doi:10.1126/science.1195591, 2010.

Junk, G. and Svec, H.: The absolute abundance of the nitrogen isotopes in the atmosphere and compressed gas from various sources, Geochim. et Cosmochim. Acta, 14, 234–243, 1958.

Kaiser, J.: Stable isotope investigations of atmospheric nitrous oxide, Ph.D. thesis, Johannes Gutenberg-Universität Mainz, 2002.

Kim, K. R. and Craig, H.: Nitrogen-15 and oxygen-18 characteristics of nitrous oxide: A global perspective, Science, 262, 1993.

5 Lewicka-Szczebak, D., Well, R., Köster, J. R., Fuß, R., Senbayram, M., Dittert, K., and Flessa, H.: Experimental determinations of isotopic fractionation factors associated with N2O production and reduction during denitrification in soils, Geochimica et Cosmochimica Acta, 134, 55–73, doi:10.1016/j.gca.2014.03.010, 2014.

Mariotti, A., Germon, J. C., Hubert, P., Kaiser, P., Letolle, R., Tardieux, A., and Tardieux, P.: Experimental determination of nitrogen kinetic isotope fractionation: some principles; illustration for the denitrification and nitrification processes, Plant and soil, 430, 413–430, 1981.

10 Menyailo, O. V. and Hungate, B. A.: Stable isotope discrimination during soil denitrification: Production and consumption of nitrous oxide, Global Biogeochemical Cycles, 20, n/a–n/a, doi:10.1029/2005GB002527, 2006.

Mosier, A., Kroeze, C., and Nevison, C.: Closing the global N2O budget: nitrous oxide emissions through the agricultural nitrogen cycle, Nutrient Cycling in Agroecosystems, 52, 225–248, 1998.

Olivier, J. G. J., Bouwman, A. F., Van der Hoek, K. W., and Berdowski, J. J. M.: Global air emission inventories for anthropogenic sources
15 of NOx, NH3, and N2O in 1990, Environmental Pollution, 102, 135–148, 1998.

Ostrom, N. E., Pitt, A., Sutka, R., Ostrom, P. H., Grandy, A. S., Huizinga, K. M., and Robertson, G. P.: Isotopologue effects during N2O reduction in soils and in pure cultures of denitrifiers, Journal of Geophysical Research, 112, G02 005, doi:10.1029/2006JG000287, 2007.

Park, S., Pérez, T., Boering, K. A., Trumbore, S. E., Gil, J., Marquina, S., and Tyler, S. C.: Can N2O stable isotopes and isotopomers be useful tools to characterize sources and microbial pathways of N2O production and consumption in tropical soils?, Global Biogeochemical
20 Cycles, 25, GB1001, doi:10.1029/2009GB003615, 2011.

Schilt, A., Baumgartner, M., Schwander, J., Buiron, D., Capron, E., Chappellaz, J., Loulergue, L., Schüpbach, S., Spahni, R., Fischer, H., and Stocker, T. F.: Atmospheric nitrous oxide during the last 140,000years, Earth and Planetary Science Letters, 300, 33–43, doi:10.1016/j.epsl.2010.09.027, 2010.

Stuart Chapin III, F., Matson, P. A., and Mooney, H. A.: Principles of terrestrial ecosystem ecology, Springer-Verlag, New York, 2002.

25 Sutka, R. L. and Ostrom, N. E.: Distinguishing nitrous oxide production from nitrification and denitrification on the basis of isotopomer abundances, Applied and environmental microbiology, 72, 638–644, doi:10.1128/AEM.72.1.638, 2006.

Tosha, T. and Shiro, Y.: Crystal structures of nitric oxide reductases provide key insights into functional conversion of respiratory enzymes, IUBMB Life, 65, 217–226, doi:10.1002/iub.1135, 2013.

Toyoda, S., Yoshida, N., Miwa, T., Matsui, Y., Yamagishi, H., and Tsunogai, U.: Production mechanism and global budget of N 2 O inferred
30 from its isotopomers in the western North Pacific, Geophysical Research Letters, 29, 5–8, 2002.

Well, R. and Flessa, H.: Isotopologue signatures of N 2 O produced by denitrification in soils, Journal of Geophysical Research, 114, G02 020, doi:10.1029/2008JG000804, 2009a.

Well, R. and Flessa, H.: Isotopologue enrichment factors of N2O reduction in soils, Rapid Communications in Mass Spectrometry, pp. 2996–3002, doi:10.1002/rcm, 2009b.

35 Wrage, N., Velthof, G. L., Beusichem, M. L. V., and Oenema, O.: Role of nitrifier er denitrication in the production of nitrous oxide, Soil Biology and Biochemistry, 33, 1723–1732, 2001.

Yoshida, N. and Toyoda, S.: Constraining the atmospheric N2O budget from intramolecular site preference in N2O isotopomers, Nature, 405, 330–4, doi:10.1038/35012558, 2000.

Biogeosciences
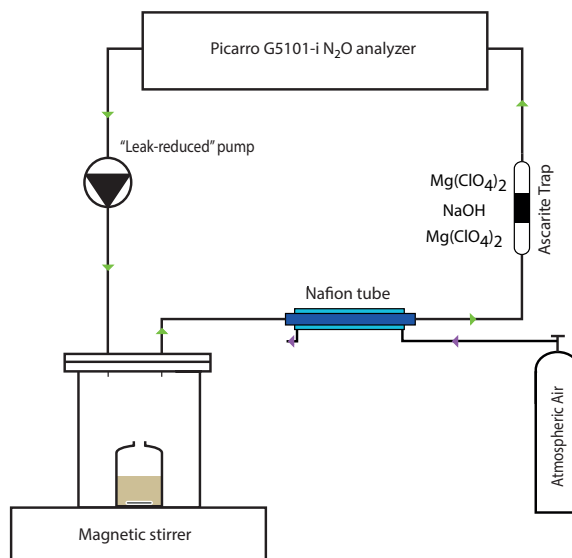Discussions

Open Access

EGU

Figure 1. Simplified schematic of the incubation setup. The green and the purple arrows show the flow direction of the measuring gas and the purge gas, respectively.
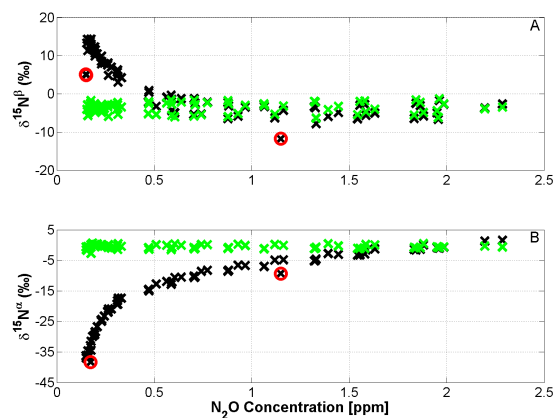

Figure 2. The concentration-dependent correction (CDC) for (A) $\delta^{15}N^{\alpha}$ and (B) $\delta^{15}N^{\beta}$ respectively. In both Figures, the raw data are presented in black, the CDC data is plotted in green, and the outliers are marked with red circles.
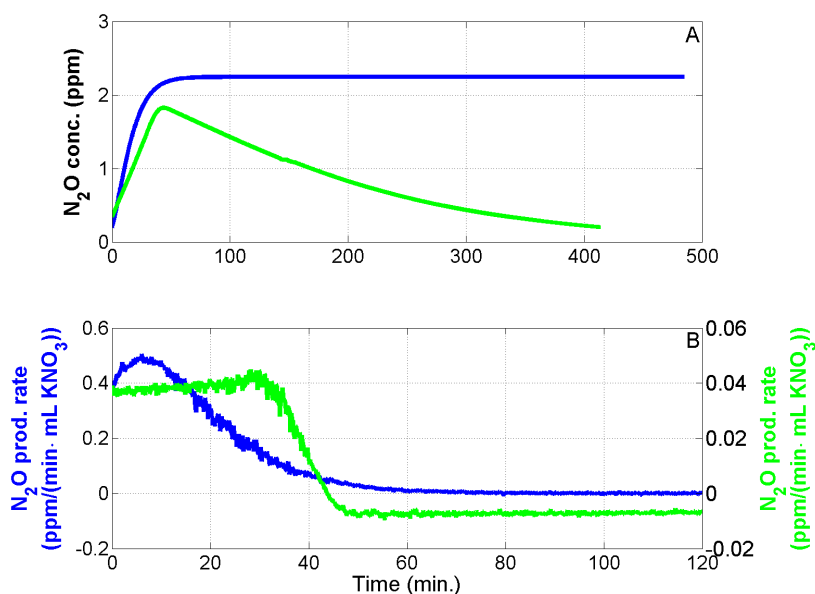
Figure 3. Continuous measurements of (A) N_2O concentrations and (B) the N_2O production rate from experiments with *P. fluorescens* (green) and *P. chlororaphis* (blue), respectively. Only the first 120 minutes of the N_2O production. Note that the scaling of the two horizontal axis differs.
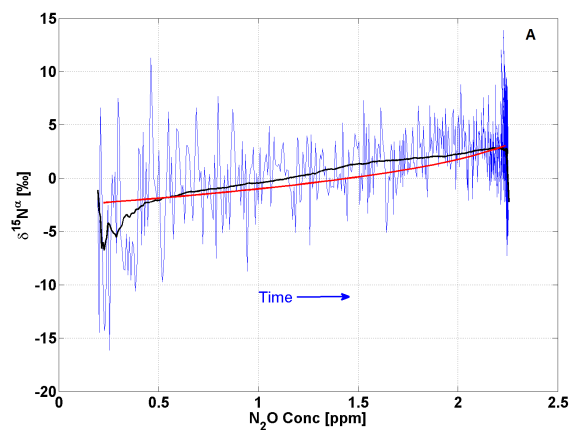

Figure 4A. The evolution of (A) the $\delta^{15}N^{\alpha}$ isotopomers evolution in relation to the concentration of N_2O and the modeled Rayleigh type distillation. The blue profile is the CDC data. The black profile is the five minutes running mean of the CDC data. The red profile is the modeled Rayleigh type distillation curve for the production of N_2O. The blue arrow indicate the direction of time.

Figure 4B. The evolution of the $\delta^{15}N^{\beta}$ isotopomers evolution in relation to the concentration of N_2O and the modeled Rayleigh type distillation. The blue profile is the CDC data. The black profile is the five minutes running mean of the CDC data. The red profile is the modeled Rayleigh type distillation curve for the production of N_2O. The blue arrow indicate the direction of time.
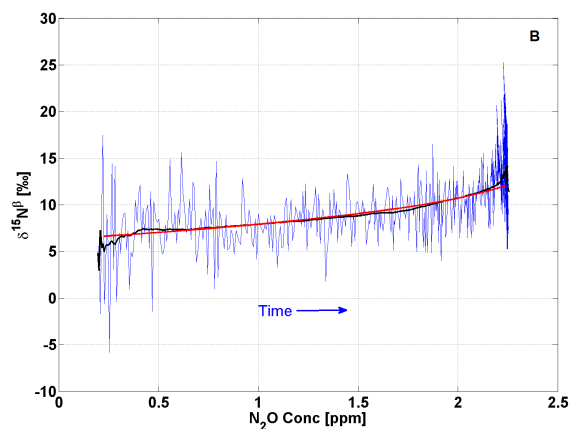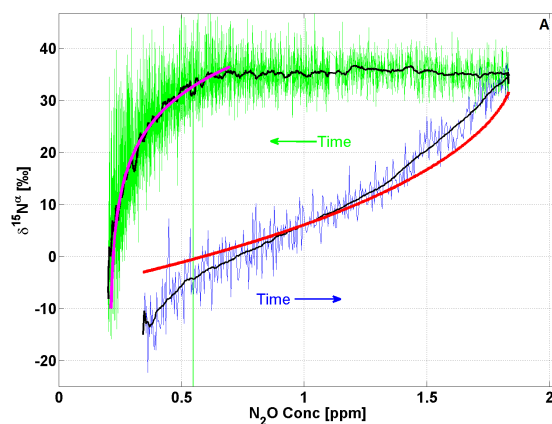

Figure 5A. The evolution of the $\delta^{15}N^{\alpha}$ isotopomers evolution in relation to the concentration of N_2O and the modeled Rayleigh type distillation. The blue profile is the CDC data. The black profile is the five minutes running mean of the CDC data. The red profile is the modeled apparent Rayleigh type distillation curve for the production of N_2O. The blue arrow indicates the direction of time during production of N_2O whereas the green arrow indicates the direction of time during reduction of N_2O.
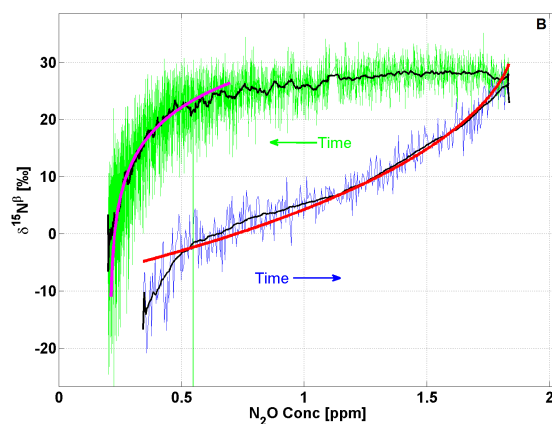
Figure 5B. The evolution of the $\delta^{15}N^{\beta}$ isotopomers evolution in relation to the concentration of N_2O and the modeled Rayleigh type distillation. The blue profile is the CDC data. The black profile is the five minutes running mean of the CDC data. The red profile is the modeled apparent Rayleigh type distillation curve for the production of N_2O. The blue arrow indicates the direction of time during production of N_2O whereas the green arrow indicates the direction of time during reduction of N_2O.
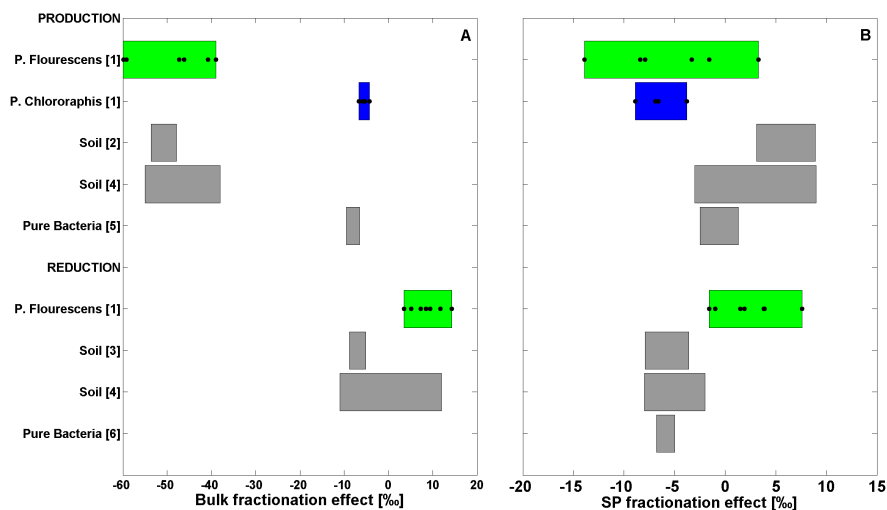

Figure 6. (A) Bulk and (B) SP enrichment factors calculated from the continuous measurements with *P. fluorescens* (green) and *P. chlororaphis* (blue) respectively. Both the production and reduction isotope enrichment values are shown and compared with previously presented results. [1] [This study], [2] [(Well and Flessa, 2009a)], [3] [(Well and Flessa, 2009b)], [4] [(Lewicka-Szczebak et al., 2014)], [5] [(Sutka and Ostrom, 2006)], [6] [(Ostrom et al., 2007)].

Table 1. Measurements of standard gas CIC-MPI-1 and CIC-MPI-2, diluted MPI-1 and MPI-2 gasses respectively. The listed values are mean-values of measurements performed at Tokyo-Tech, IMAU, and CIC.

Reference gas	[N$_2$O] (ppb)	$\delta^{15}N^{bulk}$ (‰)	$\delta^{15}N^{\alpha}$ (‰)	$\delta^{15}N^{\beta}$ (‰)
CIC-MPI-I	1904.0 ± 9.2	1.23 ± 1.97	1.45 ± 2.09	1.01 ± 1.85
CIC-MPI-II	1840.9 ± 12.8	-1.69 ± 1.74	12.02 ± 1.78	-15.40 ± 1.69

Table 2. Enrichment factors for the production of N$_2$O from *P. fluorescens*.

Replica #	ϵ_{α} (‰)	ϵ_{β} (‰)	ϵ_{bulk} (‰)	ϵ_{SP} (‰)
1	-64.1	-55.7	-59.9	-8.4
2	-41.6	-40.0	-40.8	-1.6
3	-45.9	-32.0	-39.0	-13.9
4	-64.7	-56.3	-60.5	-8.4
5	-51.2	-43.3	-47.3	-7.9
6	-60.8	-57.5	-59.2	-3.3
7	-44.5	-47.8	-46.2	3.3
Mean	**-53.3 ± 9.8**	**-47.5 ± 9.7**	**-50.4 ± 9.3**	**-5.7 ± 5.6**

Table 3. Enrichment factors for the reduction of N$_2$O from *P. fluorescens*.

Replica #	ϵ_{α} (‰)	ϵ_{β} (‰)	ϵ_{bulk} (‰)	ϵ_{SP} (‰)
1	10.0	8.1	8.5	1.9
2	3.5	4.5	3.5	-1.0
3	11.9	8.1	9.4	3.8
4	4.6	6.2	5.1	-1.6
5	16.3	8.7	11.7	7.6
6	16.9	13.0	14.3	3.9
7	9.8	8.3	7.3	1.5
Mean	**10.4 ± 5.2**	**8.1 ± 2.6**	**8.5 ± 3.7**	**2.3 ± 3.2**

Table 4. Enrichment factors for the production of N_2O from *P. chlororaphis*.

Replica #	ϵ_{α} (‰)	ϵ_{β} (‰)	ϵ_{bulk} (‰)	ϵ_{SP} (‰)
1	-10.4	-1.5	-6.0	-8.9
2	-7.7	-0.8	-4.3	-6.9
3	-8.7	-2.1	-5.4	-6.6
4	-7.2	-3.4	-5.3	-3.8
5	-10.0	-3.3	-6.7	-6.7
Mean	**-8.8 ± 1.4**	**-2.2 ± 1.1**	**-5.5 ± 0.9**	**-6.5 ± 1.8**